Chemical Engineering Journal 156 (2010) 184–192

Contents lists available at ScienceDirect

Chemical Engineering Journal

journal homepage: www.elsevier.com/locate/cej

Pores occlusion in MCM-41 spheres immersed in SBF and the effect on ibuprofen delivery kinetics: A quantitative model

Renato Mortera [b], Sonia Fiorilli [b], Edoardo Garrone [b], Enrica Verné [a], Barbara Onida [b,*]

[a] Dipartimento di Scienza dei Materiali ed Ingegneria Chimica, Politecnico di Torino, Corso Duca degli Abruzzi 24, 10129 Torino, Italy
[b] CR-INSTM for Materials with Controlled Porosity, Italy

ARTICLE INFO

Article history:
Received 21 May 2009
Received in revised form
24 September 2009
Accepted 6 October 2009

Keywords:
Ordered mesoporous silica
Drug delivery
MCM-41 spheres
Release kinetics

ABSTRACT

MCM-41 silica particles have been synthesized with size in the low submicron range, loaded with ibuprofen and characterized by means of XRD, N_2 adsorption and scanning electron microscopy, coupled with EDS analysis both before and after contact with different volumes of simulated body fluid (SBF) at 37 °C up to 10 h.

The particles do not show any change in morphology, composition and mesostructure as a consequence of soaking. MCM-41 spheres, though, are not inert towards SBF. Two processes take place, showing features independent from the soaking volume: (i) one within 1–2 h, bringing about dissolution of silica into the liquid phase up to a concentration of 2.2 mM and no change in the mesopore volume; (ii) the second, after an induction period of 1–2 h, bringing about a limited increase in the concentration of dissolved silica, but affecting severely the mesoporous volume, which decreases exponentially with time.

Delivery curves differ significantly when varying the volume of SBF used. To account for release kinetics under the circumstances observed, a mathematical model is proposed, based on the standard Noyes–Whitney equation, taking into account both the SBF volume used and the mesopores occlusion, this latter through a time-dependent diffusion coefficient. A satisfactory agreement is observed, without the intervention of any adjustable parameter.

1. Introduction

Ordered mesoporous silicas have been proposed for the first time as carriers for drug delivery in 2001 by Vallet-Regí et al. [1] Their narrow pore size distribution and their high specific surface area [2], in combination with the possibility to modulate the pore diameter in a wide range by varying synthesis conditions, made these materials widely investigated for the incorporation and the release of pharmaceutical agents.

Several studies have been carried out on the system proposed in 2001, and several other mesoporous silicas have been suggested as matrices for drug delivery systems, especially for non-steroidal anti-inflammatory drugs [3–15]. In 2003 Tourne-Peteilh et al. [16] proposed the functionalization of the hexagonal mesostructure MCM-41 with 3-glycidoxypropylsilane in order to obtain a covalent bond between the drug and the silica walls, and Lin and co-workers [17] synthesized MCM-41 nanoparticle-based stimuli-responsive systems using a concept of gatekeeping. Recently new designs have been proposed for MCM-41 silica, i.e. the luminescent functionalization of the pore walls [18,19], the magnetic particles inclusion into the mesopore channels [20,21] and the inner pore surface modification to affect the drug release [22–24].

Since 2004, the *in vitro* studies of the mesoporous silica endocytosis into various cell types have pointed out that the biocompatibility of these systems is fairly high [9,25–27]. In addition, Slowing et al. [28] reported no haemolysis of mammalian red blood cells in contact with MCM-41 nanoparticles, indicating their possible intravenous administration and transport.

The use of ordered mesoporous silicas has been studied in the context of bone tissue engineering [29–31], also in combination with bioactive glass–ceramic scaffolds [32–34]. In this field the possibility of delivering in a predetermined way drugs after surgical treatments or fractures is crucial to avoid the side effects of the current therapies based on large amounts of antibiotics and anti-inflammatory drugs.

Among the various molecules tested, ibuprofen (IBU) was extensively adopted as model drug to characterize up-take capacity and release properties of different systems, especially in contact with the solution commonly used for the *in vitro* simulation of body fluid (SBF) [35]. Moreover, IBU dosed in appropriate concentration decreases the side effects on bone formation of the current heal-

* Corresponding author. Tel.: +39 0115644631; fax: +39 0115644699.
E-mail address: barbara.onida@polito.it (B. Onida).

1385-8947/$ – see front matter © 2009 Elsevier B.V. All rights reserved.
doi:10.1016/j.cej.2009.10.018

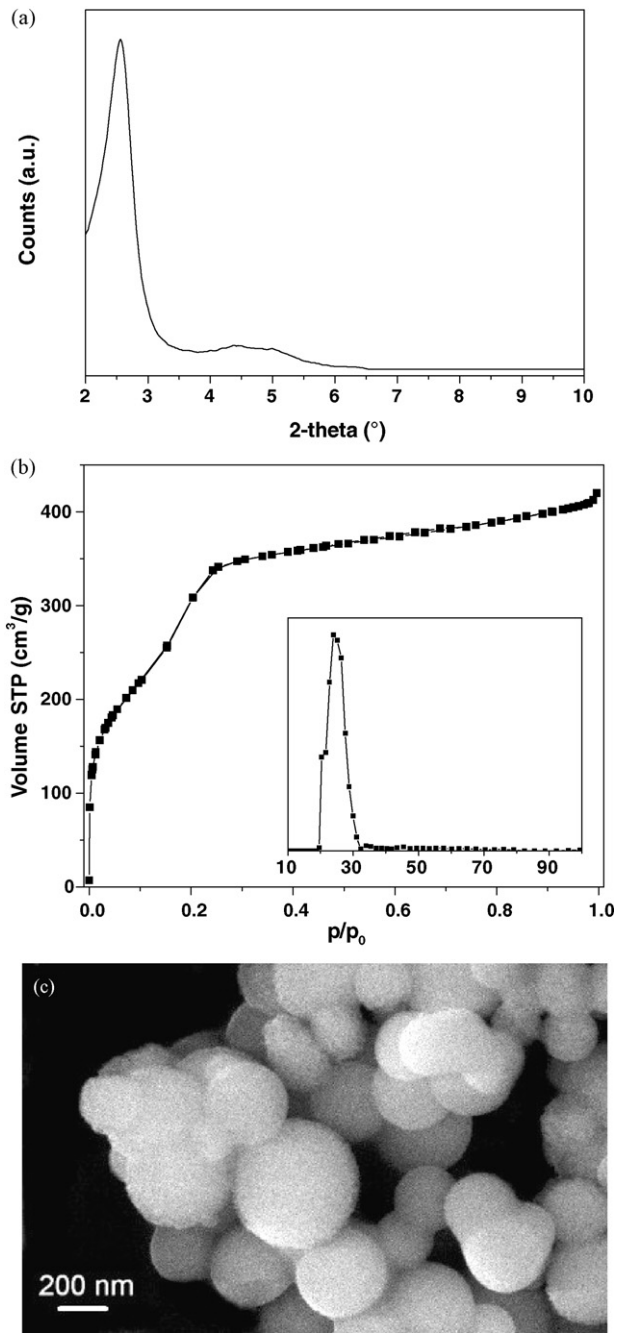

Fig. 1. XRD pattern (a), nitrogen adsorption–desorption isotherms at 77 K with DFT pore size distribution ((b), inset) and SEM picture (c) of calcined MSP.

ing prophylaxis based on non-steroidal anti-inflammatory drugs [36,37].

Although it has been reported that sol–gel silica may degrade during the contact with biological fluids [38–40], the few data available on mesoporous silica tablets showed a small extent of dissolution [4]. For this reason, several attempts to model the IBU release kinetics from ordered mesoporous silicas are based on the assumption that the silica matrix is insoluble and behaves as an inert porous carrier [12,30]. In contrast Andersson et al. [4] hypothesized a possible correlation between drug release and silica dissolution. Also, IBU release curves in SBF from MCM-41 silicas with pore diameter around 2.5 nm, similar to those adopted in the present study, have shown a peculiar discontinuity [6,33,41], ascribed to occlusion of mesopores occurring during contact with SBF [42].

Table 1
Specific surface area (SSA), mesopore volume (V_p), pore size (D_{DFT}) and d_{100} values for MSP after different immersion times in SBF at 37 °C.

	N_2 adsorption–desorption			XRD
	SSA_{BET} (m^2/g)	V_p (cm^3/g)	D_{DFT} (nm)	d_{100} (nm)
MSP	835	0.548	2.4	3.45
MSP-30 (1.0 h)	829	0.549	2.4	3.47
MSP-30 (1.5 h)	741	0.394	2.5	3.46
MSP-30 (2.0 h)	440	0.234	2.5	3.43
MSP-30 (6.0 h)	38	0.012	–	3.44
MSP-30 (8.0 h)	15	0.007	–	3.43
MSP-30 (10.0 h)	16	0.007	–	3.47

The present paper reports a detailed study of MCM-41 spheres, as it concerns their behaviour in SBF, under different IBU release conditions, in order to assess whether these materials may be really considered inert.

The aim of the study is twofold. On the one hand, a complete characterization of MCM-41 mesopores occlusion process in SBF may be crucial to develop MCM-41-based systems for *in vivo* applications. On the other hand, the investigation of the variations of IBU delivery profile upon changing the SBF contact volume may be useful to model the release features in different biological conditions.

2. Experimental

2.1. Synthesis of MCM-41 spheres

MCM-41 spheres were prepared according to the procedure reported by Grün et al. [43], slightly modified in that a lower pH value was assumed in the synthesis [33].

2.5 g n-hexadecyltrimethylammonium bromide (C_{16}TMABr, Aldrich) was dissolved into a mixture composed by 50 g deionized water, 0.15 g aqueous ammonia (33 wt.%, Riedel-de Häen) and 60 g absolute ethanol (99.9% Labochem). 4.7 g tetraethylorthosilicate (TEOS 98%, Aldrich) were then added. The reactant molar ratio was therefore: 1TEOS:0.3C_{16}TMABr:0.129NH_3:144H_2O:58EtOH. After stirring for 2 h at room temperature, the product was filtered, dried overnight at 90 °C and calcined at 550 °C for 6 h in flowing dry air (heating rate: 1 °C/min).

2.2. Drug up-take

Adsorption of IBU (99.9%, Sigma) has been carried out by contacting a pentane solution (10 ml, 33 mg/ml, 0.160 M) with 400 mg of MCM-41 spheres for 2 h at room temperature under

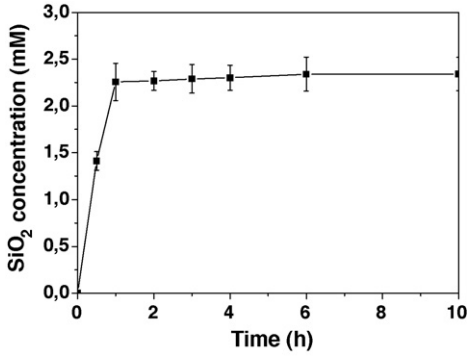

Fig. 2. Concentration of dissolved silica measured for MSP soaked in 30 ml of SBF (MSP-30) at 37 °C.

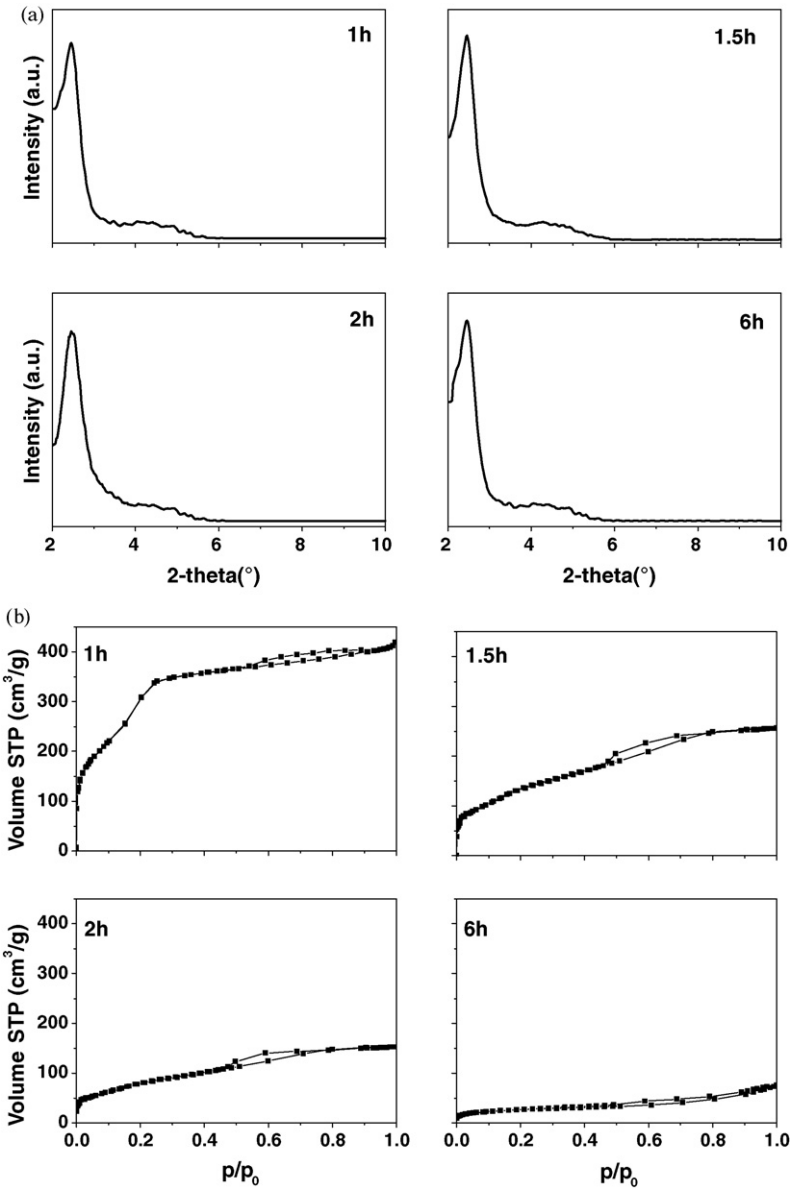

Fig. 3. XRD patterns (a) and nitrogen adsorption–desorption isotherms at 77 K (b) of MSP-30 obtained after different immersion times in SBF at 37 °C.

continuous stirring. The amount of drug loaded was evaluated through UV–vis spectrophotometry from the change in concentration in the pentane solution. The instrument was a Cary 500 Scan, operating at $\lambda = 263$ nm, where the molar extinction coefficient (ε_λ) is 320 $mol^{-1}\,cm^{-1}$. The calibration curve has been drawn using pentane solutions of IBU in the same concentration range.

The as-synthesized and the IBU-loaded MCM-41 mesoporous silica particles are hereafter referred to MSP and MSP-IBU, respectively.

2.3. Drug release and MSP behaviour in SBF

The drug release kinetics were evaluated *in vitro* by soaking the same amount of MSP-IBU (100 mg) in different volumes (ranging from 10 ml to 210 ml) of stirred SBF kept at 37 °C. The number representing the volume used in milliliter features last in the acronym: e.g. MSP-IBU-30 indicates 100 mg of MSP-IBU soaked in 30 ml of SBF.

At different time intervals, a small amount of SBF (0.1 ml) was collected and analysed through UV–vis spectrophotometry to assess the amount of released IBU. In SBF the maximum wavelength is still at $\lambda = 263$ nm, but ε_λ is equal to 440 $mol^{-1}\,cm^{-1}$.

In a parallel set of experiments, 100 mg of IBU-free MSP samples have been soaked directly in different volumes of SBF at 37 °C (the related acronym being MSP-*X*, *X* referring to the SBF volume in milliliter). The amount of silica dissolved in SBF was measured using molybdenum blue as a tracer and the concentration was monitored by means of UV–vis spectrophotometry ($\lambda = 410$ nm) [4,44].

2.4. Characterization

The samples have been characterized by means of powder X-ray diffraction (X'Pert Philips, CuK_α radiation), nitrogen adsorption/desorption measurements at 77 K (Quantachrome Autosorb1) and field emission scanning electron microscopy (Assing FESEM Supra 25) associated with energy dispersive spectroscopy (EDS, Oxford Instrument INCA X-Sight). Characterization has been car-

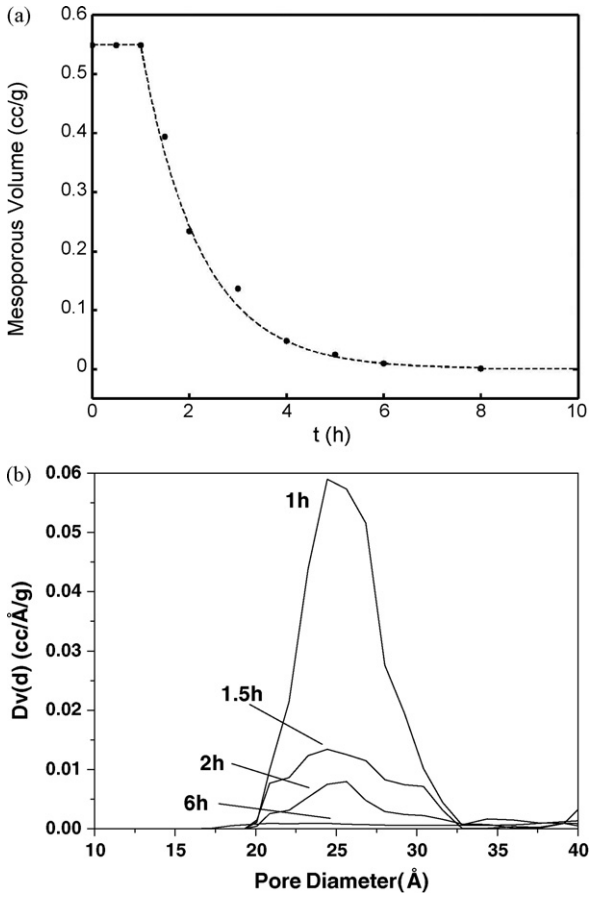

Fig. 4. Trend of mesoporous volume (a) and pore size distributions (b) of MSP-30 during the contact with SBF at 37 °C.

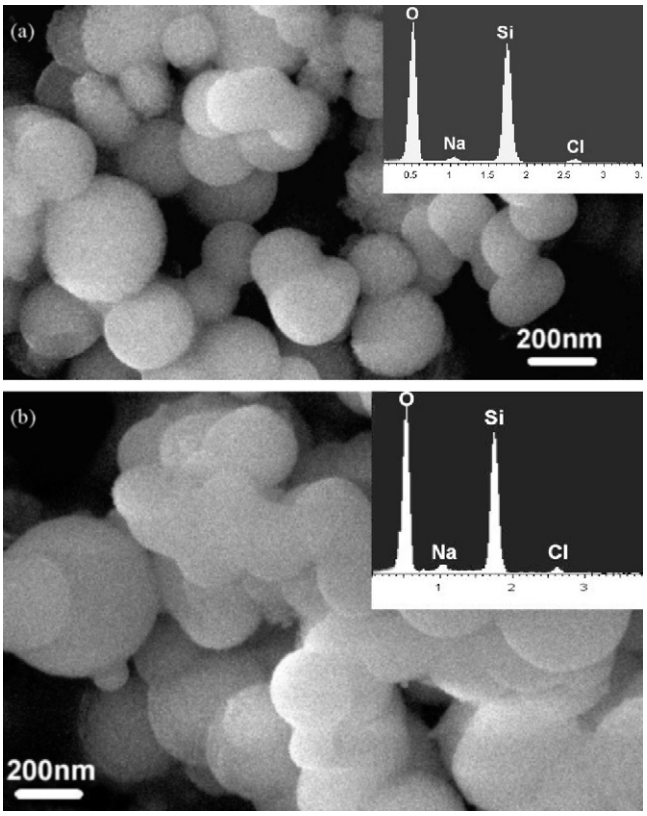

Fig. 5. SEM pictures and EDS analysis (inset) of MSP-30 after 1 h (a) and 6 h (b) of immersion in SBF at 37 °C.

ried out both on MCM-41 as such and after immersion in SBF for different times. Before nitrogen adsorption/desorption measurements, each sample has been outgassed at room temperature for 6 h.

Pore size has been evaluated through the DFT method, using the NLDFT equilibrium model for cylindrical pore [45].

3. Results and discussion

3.1. MCM-41 spheres

XRD pattern of MSP shows the typical peak due to the (1 0 0) reflection of the ordered 2D hexagonal mesostructure at 2θ value of 2.56° (Fig. 1a). The corresponding d_{100} results 3.45 nm (Table 1). The (1 1 0) and (2 0 0) reflections appear ill-defined at 2θ values of 4.44° and 5.02°, respectively. Lowering the synthesis pH with respect the value reported by Grün et al. [43] causes a broadening of d_{110} and d_{200} peaks. This is ascribed to a lower mesoscopic order, because a lower alkalinity usually favours the formation of disordered phases [46]. The cell parameter (a), calculated as $a = (2/\sqrt{3})d_{100}$, results to be 3.98 nm.

Fig. 1b reports nitrogen adsorption/desorption isotherms of calcined MSP. These are of type IV, and exhibit filling of the mesopores at relative pressure p/p^0 below 0.3. The values of BET specific surface area and mesopores volume are 835 m^2/g and 0.55 cm^3/g, respectively (Table 1). Pore diameter, as evaluated by DFT model (N_2 on SiO_2 kernel, fitting error = 0.65%), results 2.4 nm (Fig. 1b, inset). From the value of cell parameter a, wall thickness turns out to be 1.58 nm. The DFT fitting is reported in Figure S1 of the supplementary information.

MCM-41 material is in the form of spheres with size ranging from 200 nm to 800 nm, similarly to what observed by Grün et al. [43] (Fig. 1c).

3.2. MSP modification in SBF

Fig. 2 reports the profile describing the silica dissolution to SBF with time for MSP-30. A relatively fast process is observed for contact times below 1 h, when the concentration of silica in the liquid phase is about 2.2 mM (corresponding to about 4% weight of initial silica). Dissolution then practically stops and the concentration in the liquid phase reaches only 2.3 mM after 10 h. The same experiments in two different volumes of SBF (10 ml and 210 ml) gave similar results (not reported).

Table 2
Ibuprofen released from MSP-IBU-*X* after different immersion times in *X* ml of SBF at 37 °C and corresponding ibuprofen concentration in solution.

	Ibuprofen released (%)			Ibuprofen concentration (mg/ml)		
	2 h	10 h	170 h	2 h	10 h	170 h
MSP-IBU-10	53	57	60	1.84	1.98	2.07
MSP-IBU-30	69	82	92	0.79	0.94	1.05
MSP-IBU-210	78	99	100	0.13	0.16	0.16

Literature data on amorphous sol–gel silica show a sizable extent of dissolution also in the first 10 h of contact with biological fluids [38–40]. No results seem to be available concerning the dissolution in SBF of dispersed mesoporous silica spheres. The few literature data on mesoporous silica tablets, containing IBU, show a smaller extent of dissolution than the sol–gel silica, but a different kinetics with respect to that here reported for MSP-30 [4].

A reason for the lower extent of dissolution observed for ordered mesoporous silicas with respect to amorphous sol–gel silica may reside in the ageing and the subsequent calcination process typical of the former systems [47].

Fig. 3a shows XRD patterns of MSP-30 after different soaking times in SBF. These do not change significantly, so showing that the mesostructure is stable during contact with SBF. A broadening of (1 1 0) and (2 0 0) reflections is observed with respect to the pattern reported in Fig. 1a, but the mesoscopic order is evident even after 6 h of soaking (Fig. 3a) [47] and the d_{100} distance does remain constant (Table 1).

Fig. 3b reports nitrogen adsorption–desorption isotherms after 1 h, 1.5 h, 2 h and 6 h of soaking. The initial isotherms show the characteristic mesopore filling at p/p^0 below 0.3 (type IV). Increasing the soaking time, the N_2 adsorbed volume decreases and the characteristic mesopore filling becomes less evident. After 6 h of soaking, isotherms do not show any longer the pore filling associated with mesopores. A hysteresis loop at p/p^0 above 0.5 is observed in all cases, probably due to the interparticle porosity [48].

The mesoporous volume remains constant at 0.55 cm^3/g during the first hour of contact with SBF, then decays, reaching 0.01 cm^3/g after 8 h, as observed in Fig. 4a and Table 1. The corresponding DFT pore size distributions (N_2 on SiO_2 kernel, fitting error = 0.65%) confirm this trend with a marked decrease of the peak intensity with soaking time. The presence of mesopores at about 2.4 nm is discernible up to 6 h of SBF contact (Fig. 4b). It is worth noting that the decrease in mesoporous volume is not accompanied by any decrease in pore diameter, which remains constant.

These data indicate a progressive occlusion of mesopores after 1 h of soaking rather than a progressive reduction of pores diameter. We ascribe this modification to dissolution of silica and re-precipitation as silica gel at the pores mouth [49,50].

The decrease in mesopore volume may be represented as an exponential with a negative time constant ($-\alpha$) equal to $-0.82\ h^{-1}$. The asymptotic value, reached after 8 h of SBF contact, is negligible (0.01 cm^3/g) and it will not be considered further.

SEM pictures of MSP-30 after 1 h (Fig. 5a) and 6 h (Fig. 5b) of soaking in SBF reveal that particles maintain their spherical shape without any remarkable variations with respect to calcined MSP (Fig. 1c). EDS analysis show the peak ascribable to silica at 1 h and at 6 h (Fig. 5, insets). The presence in both cases of traces of sodium chloride is due to residues coming from SBF solution.

MSP-10 and MSP-210 exhibit a very similar occlusion of mesopores during their contact with SBF (Figure S2 of the supplementary information), so showing a behaviour that seems to be independent from the soaking volume.

3.3. Drug up-take and release

The amount of IBU adsorbed by MSP-IBU is about 34.7% (w/w) (hereafter referred to as I_L), in good agreement with the literature [6,51–53].

Fig. 6 shows the kinetics of IBU release from 100 mg of MSP-IBU to 10 ml, 30 ml and 210 ml, respectively, of stirred SBF maintained at 37 °C. Data in Fig. 6a are expressed as the concentration of ibuprofen in SBF as a function of time and refer to the first 10 h of release, whereas in Fig. 6b, the percentage of IBU released is considered.

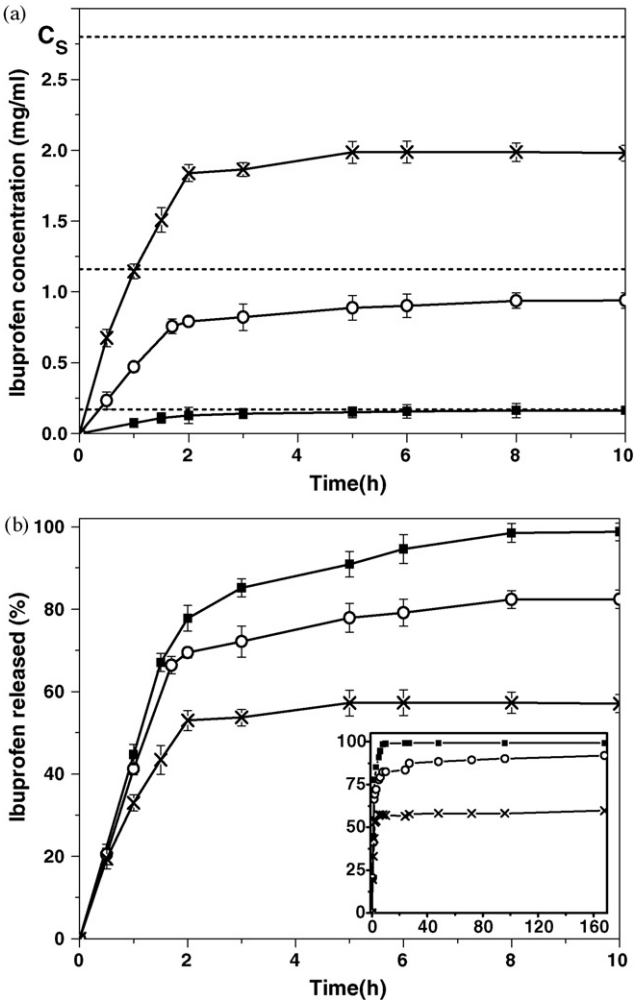

Fig. 6. Kinetics of ibuprofen release from 100 mg of MSP-IBU to 10 ml (×), 30 ml (○) and 210 ml (■) of stirred SBF maintained at 37 °C: concentration of ibuprofen in SBF (a) and amount released (b). The first 10 h of release are depicted in detail while the profiles up to 170 h are reported as inset in (b).

The amount of ibuprofen in the solid phase is 34.7 mg, equivalent to 1.6×10^{-4} moles. Assuming the total release from the solid phase, it can be anticipated that the limit value for the concentration in 210 ml, 30 ml and 10 ml of solution should be 0.16 mg/ml, 1.16 mg/ml and 3.47 mg/ml respectively. This latter value cannot be reached because the solubility of ibuprofen in SBF (C_S) is 2.8 mg/ml [54]. Fig. 6a shows, however, that only in the case of MSP-IBU-210 the concentration of released ibuprofen reaches the expected values. The three release profiles differ significantly: after 10 h MSP-IBU-10 released about 57% of incorporated drug, whereas about 82% and about 100% of ibuprofen was released from MSP-IBU-30 and from MSP-IBU-210, respectively (Table 2 and Fig. 6b).

It is worth noting that the release curve of MSP-IBU-30 corresponds to the conditions commonly used in literature and presents the trend reported for MCM-41 with pore size around 2.5 nm [6,33,41,42,53].

In order to evidence possible pores occlusion during ibuprofen release, N_2 adsorption–desorption isotherms and X-ray diffraction patterns of MSP-IBU-210, MSP-IBU-30 and MSP-IBU-10 after 2 h and 6 h of SBF contact have been collected. Results are reported in Fig. 7.

Whereas XRD patterns (inset) confirm the stability of the mesoporous structure, N_2 physisorption data show for all samples an

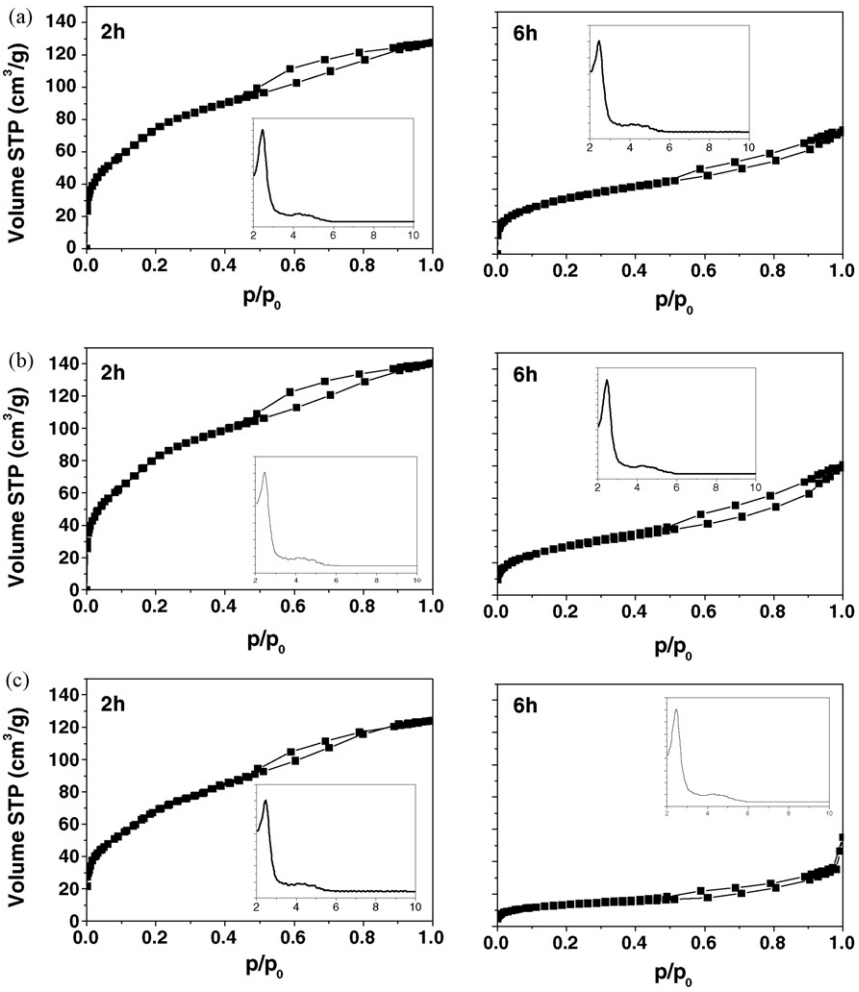

Fig. 7. Nitrogen adsorption–desorption isotherms at 77 K and X-ray diffraction patterns (insets) of MSP-IBU-210 (a), MSP-IBU-30 (b) and MSP-IBU-10 (c) obtained after 2 h and 6 h of contact with SBF at 37 °C.

occlusion of mesopores similar to that observed for MSP without IBU, independently from the volume of the liquid phase. Indeed, the characteristic rise in adsorbed amount (mesopore filling) at p/p^0 slightly below 0.3 is visible only with samples up to 2 h of soaking whereas it is not observed in isotherms collected after 6 h. In this case the evaluation of the silica mesoporous volume at different soaking times is not rigorous because of the presence of a time-dependent IBU amount inside mesopores. Nevertheless, data obtained by N_2 physisorption strongly suggest that the occlusion process is similar to that reported in Fig. 4 for drug-free MSP.

These results evidence that the release conditions (volume of liquid) and the mesopores occlusion play a crucial role on the IBU release kinetics. Therefore in order to model it, it is necessary to consider not only the pore diameter, as usually reported in literature [55], but also the volume of SBF used for the release study and the changes of the mesoporous silica matrix with time. Of these latter two aspects, the former is rather obvious, though not always considered; the latter is instead new, and deserves particular attention.

The use of Noyes–Whitney (NW) equation (Eq. (1)) to describe the dissolution of a drug confined in inert porous carriers is widely reported in literature [56–58]: its application for IBU release from ordered mesoporous silica was proposed by Vallet-Regí et al. [12,30], assuming the delivery as independent of the volume of the liquid phase, since taking place under vigorous stirring.

It is appropriate to recall that the NW model was originally proposed for dissolution kinetics. The flow of matter from the solid to the solution is therefore proportional to the difference between C_t, concentration of the solution in contact with the solid solute (here the mesoporous solid), and the concentration at saturation C_S in SBF at 37 °C (2.8 mg/ml).

The ordinary NW in its general form can be written as follows:

$$\frac{dC_t}{dt} = K(C_S - C_t) \quad (1)$$

K is the proportionality constant, which using Fick's first law, results to be [59]:

$$K = k_d \frac{A_0}{V} = \frac{DA_0}{hV} \quad (2)$$

where $k_d = D/h$ is the dissolution rate constant, D is the diffusion coefficient, h is the diffusion layer thickness, V is the volume of SBF used for the release test (ranging between 10 ml and 210 ml) and A_0 is the surface accessible to diffusion. This latter parameter was assumed as the surface separating the internal mesoporous volume of the MCM-41 particle and the external volume of the solution, as schematically depicted in Fig. 8a. Therefore A_0 has been calculated dividing the MSP mesoporous volume (0.55 cm^3/g, Table 1) by the length of the mesopores, assuming spherical particles with the same diameter (the value used was 400 nm, as obtained from SEM data) and a radial disposition of the cylindrical mesopores [60]

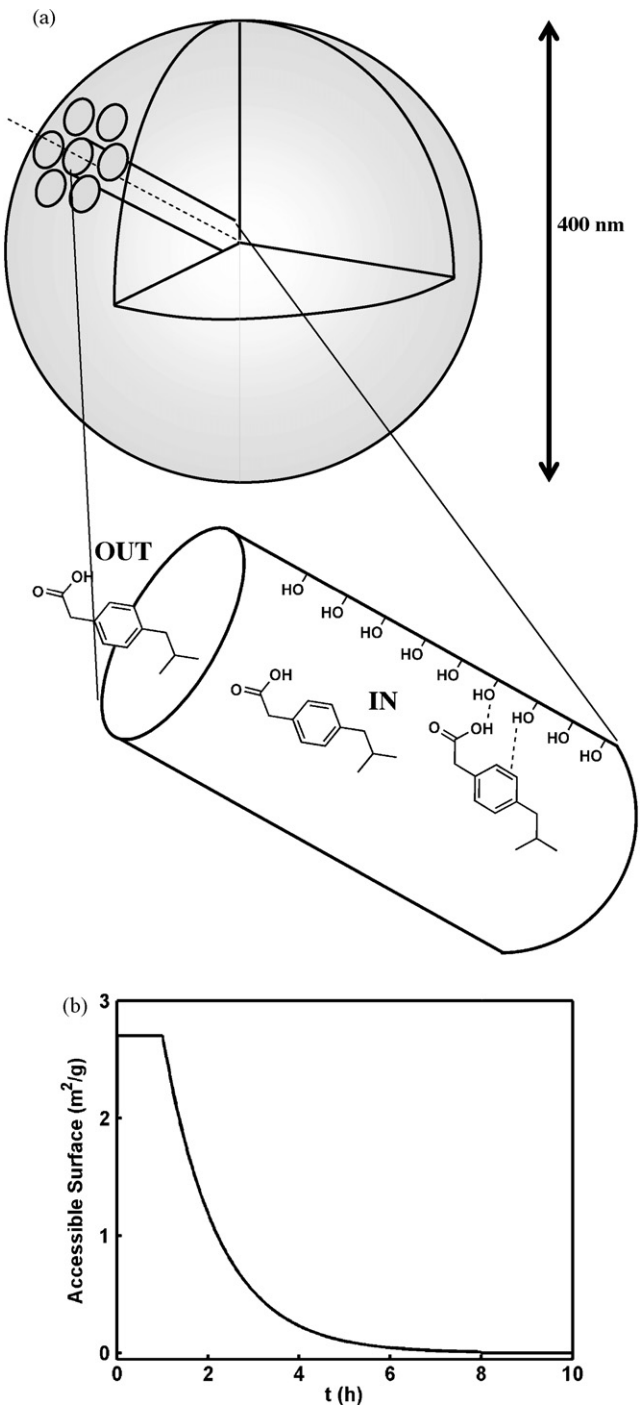

Fig. 8. Radial disposition of the cylindrical mesopores inside the silica spheres with a mean diameter of 4070 nm (a) Trend of the accessible surface (A(t)) during the first 10 h of contact with SBF at 37 °C (b).

(Table 3). D has been determined using the Stokes–Einstein equation to derive the IBU diffusivity for the plasma (D_{pl}) and the Renkin equation to correct the value with the sterical hindrance (δ) and the constrictivity (ω_r) [55]:

$$D = D_{pl}\frac{\delta\varpi_r}{\tau} = D_{pl}\frac{(1-a/r)^2(1-2.1(a/r)+2.09(a/r)^3-0.95(a/r)^5)}{\tau} \quad (3)$$

δ and ω_r are both functions of the ratio between the IBU and the pore radii (a/r) and τ is the tortuosity, assumed equal to one, since the

Table 3
List of constants and parameters used in the standard and modified Noyes–Whitney simulation of ibuprofen release from MSP-IBU to different volumes of SBF.

		Value
Saturation solubility	C_S	2.8 mg/ml
Ibuprofen radius	a	0.5 nm
Mesopores radius	r	1.2 nm
Diffusion coefficient	D	8.8×10^{-8} cm^2/h
Dissolution rate constant	k_d	0.0022 cm/h
Accessible surface at $t = 0$ h	A_0	27.00 cm^2/mg
Weight of MSP-IBU sample	P	100 mg
Ibuprofen adsorbed by MSP-IBU	I_L	34.7%
Time constant	α	0.82 h^{-1}

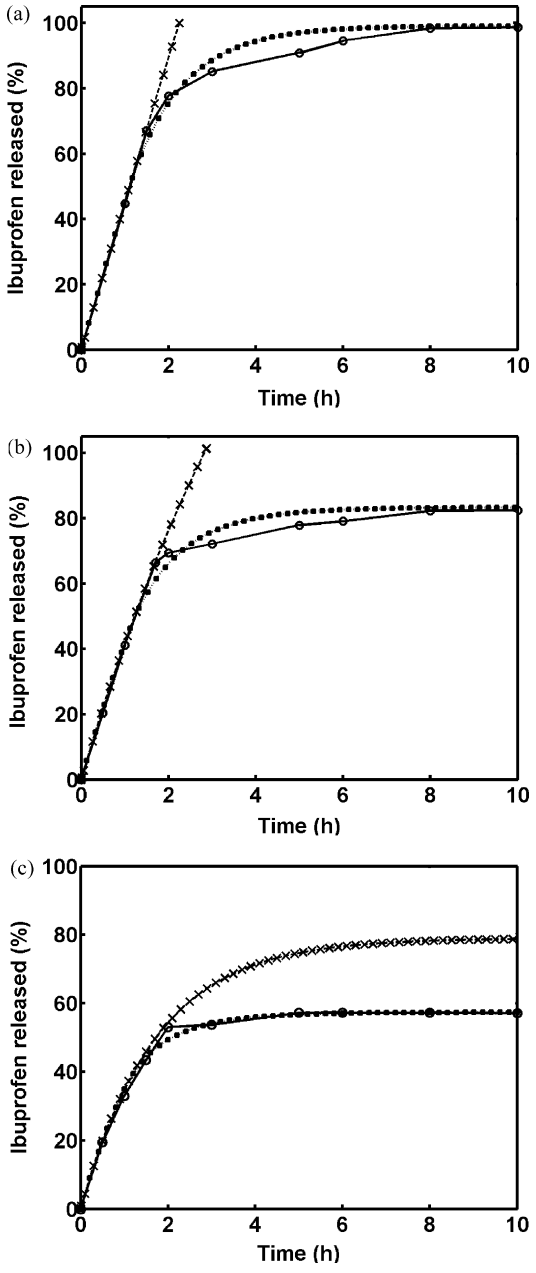

Fig. 9. Ibuprofen release kinetics of MSP-IBU-210 (a), MSP-IBU-30 (b) and MSP-IBU-10 (c) during the first 10 h of contact with SBF at 37 °C (○), compared with the simulation using the Noyes–Whitney standard (×) and modified (■) equations.

mesopores are supposed cylindrical [55]. k_d was calculated dividing D by the diffusion layer thickness (h), here assumed to coincide with the mesopores length [12]. The obtained value (0.0022 cm/h) is in agreement with what reported in literature for similar systems [12,54].

Forcing $C_t(0) = 0$, Eq. (1) yields:

$$C_t = C_S(1 - e^{-Kt}) \tag{4}$$

In terms of release as fraction of adsorbed drug, it results:

$$W_t = C_t \frac{V}{PI_L} \tag{5}$$

where P is the weight of the MSP-IBU sample used for the release and I_L is the percentage amount of ibuprofen adsorbed by MSP-IBU.

To model the progressive occlusion of the mesopores, the proportionality constant K has to be replaced with a time-dependent coefficient $K(t)$:

$$\frac{dC_t}{dt} = K(t)(C_S - C_t) \tag{6}$$

The time-dependent part of $K(t)$ is the accessible surface to diffusion $A(t)$, calculated on the basis of the exponential decay of the mesoporous volume starting after 1 h of contact with SBF, as reported in Fig. 4a and Table 1.

Taking into account the occurrence of a process affecting the mesopore volume, only after 1 h, $K(t)$ can be written as:

$$K(t) = \frac{D}{hV}A(t) \Rightarrow \begin{cases} K(t) = \dfrac{D}{hV}A_0 & t \le 1\,h \\ K(t) = \dfrac{D}{hV}A_0 e^{-\alpha(t-1)} & t > 1\,h \end{cases} \tag{7}$$

α being the time constant describing the exponential decay of the accessible surface area (Fig. 8b). The NW equation results:

$$\begin{cases} \dfrac{dC_t}{dt} = K(C_S - C_t) & t \le 1\,h \\ \dfrac{dC_t}{dt} = (Ke^{-\alpha(t-1)})(C_S - C_t) & t > 1\,h \end{cases} \tag{8}$$

Forcing $C_t(0) = 0$ and $C_t(1) = C_S(1-e^{-K})$, the solution for Eq. (8) is:

$$\begin{cases} C_t = C_S(1 - e^{-Kt}) & t \le 1\,h \\ C_t = C_S(1 - e^{(K/\alpha)e^{-\alpha(t-1)} - K((1+\alpha)/\alpha)}) & t > 1\,h \end{cases} \tag{9}$$

Eqs. (9) and (4) obviously coincide up to 1 h of release when no mesopore occlusion occurred, and diverge when the effect of mesopores occlusion becomes prevalent.

The comparison between the experimental IBU release kinetics of MSP-IBU-210, and the trends predicted by the standard NW model (1) and the modified one (8) is reported in Fig. 9a. After 1 h of immersion in SBF, as expected, the standard NW equation yields poor results. It is instead noticeable that the modified NW (square) yields a satisfactory prediction of the experimental profile.

A similar behaviour is observed for MSP-IBU-30 (Fig. 9b). Only the modified simulation profile fits satisfactorily the experimental data, whereas the standard NW equation diverges after the first hour and indicates a total delivery of the adsorbed IBU in 3 h.

The different time needed for total delivery predicted by the NW standard equation in the two cases comes from the different SBF volumes considered.

Fig. 9c shows the experimental and the simulated release curves for MSP-IBU-10. As for the previous cases, the modified NW equation approximates the whole experimental profile, whereas the standard equation gives a good fitting only up to 1 h. At variance with what discussed previously, in this case, due to the lower volume, the standard equation predicts that the concentration of released ibuprofen reaches C_S before 10 h of immersion.

4. Conclusions

Two processes seem to be involved as it concerns the soaking of MCM-41 silica powders in SBF, one consisting in the solubilisation of up to 4% of silica, but not affecting the mesopore volume, the other not really releasing silica into SBF but causing the pore blocking.

The release profiles from IBU-loaded MCM-41 particles differ significantly as a function of the volume of SBF used for the delivery test, in agreement with the description of the release process in terms of the classical NW equation.

This latter accounts for the release kinetics for all values of SBF volume only for release times shorter than 1 h. For longer times, due to occlusion of mesopores, the proportionality constant of the standard NW equation is replaced by a time-dependent coefficient. A fair agreement with experimental data up to 10 h of release has been obtained, without the use of any adjustable parameters.

This result suggests the possibility of predicting the drug delivery from MSP silica particles to different amounts of SBF, thus mimicking different biological situations and different pathological requirements.

Acknowledgements

The authors would like to thank Regione Piemonte (project Nanosafe) for financial support.

Appendix A. Supplementary data

Supplementary data associated with this article can be found, in the online version, at doi:10.1016/j.cej.2009.10.018.

References

[1] M. Vallet-Regí, A. Ramila, R.P. del Real, J. Perez-Pariente, Chem. Mater. 13 (2001) 308.
[2] C.T. Kresge, M.E. Leonowicz, W.J. Roth, J.C. Vartuli, J.S. Beck, Nature 359 (1992) 710.
[3] C. Tourne-Peteilh, D.A. Lerner, C. Charnay, L. Nicole, S. Begu, J.M. Devoisselle, Chemphyschem 4 (2003) 281.
[4] J. Andersson, J. Rosenholm, S. Areva, M. Linden, Chem. Mater. 16 (2004) 4160.
[5] G. Cavallaro, P. Pierro, F.S. Palumbo, F. Testa, L. Pasqua, R. Aiello, Drug Deliv. 11 (2004) 41.
[6] P. Horcajada, A. Ramila, J. Perez-Pariente, M. Vallet-Regí, Micropor. Mesopor. Mater. 68 (2004) 105.
[7] F.Y. Qu, G.S. Zhu, H.M. Lin, W.W. Zhang, J.Y. Sun, S.G. Li, S.L. Qiu, J. Solid State Chem. 179 (2006) 2027.
[8] T.H. Chung, S.H. Wu, M. Yao, C.W. Lu, Y.S. Lin, Y. Hung, C.Y. Mou, Y.C. Chen, D.M. Huang, Biomaterials 28 (2007) 2959.
[9] J. Lu, M. Liong, J.I. Zink, F. Tamanoi, Small 3 (2007) 1341.
[10] I.I. Slowing, B.G. Trewyn, V.S.Y. Lin, J. Am. Chem. Soc. 129 (2007) 8845.
[11] V. Cauda, B. Onida, B. Platschek, L. Muhlstein, T. Bein, J. Mater. Chem. 18 (2008) 5888.
[12] M. Manzano, V. Aina, C.O. Arean, F. Balas, V. Cauda, M. Colilla, M.R. Delgado, M. Vallet-Regí, Chem. Eng. J. 137 (2008) 30.
[13] E. Ruiz-Hernandez, A. Lopez-Noriega, D. Arcos, M. Vallet-Regí, Solid State Sci. 10 (2008) 421.
[14] B.G. Trewyn, J.A. Nieweg, Y. Zhao, V.S.Y. Lin, Chem. Eng. J. 137 (2008) 23.
[15] S.B. Wang, Micropor. Mesopor. Mater. 117 (2009) 1.
[16] C. Tourne-Peteilh, D. Brunel, S. Begu, B. Chiche, F. Fajula, D.A. Lerner, J.M. Devoisselle, New J. Chem. 27 (2003) 1415.
[17] C.Y. Lai, B.G. Trewyn, D.M. Jeftinija, K. Jeftinija, S. Xu, S. Jeftinija, V.S.Y. Lin, J. Am. Chem. Soc. 125 (2003) 4451.
[18] P.P. Yang, Z.W. Quan, C.X. Li, X.J. Kang, H.Z. Lian, J. Lin, Biomaterials 29 (2008) 4341.
[19] J.L. Vivero-Escoto, I.I. Slowing, C.W. Wu, V.S.Y. Lin, J. Am. Chem. Soc. 131 (2009) 3462.
[20] E. Ruiz-Hernandez, A. Lopez-Noriega, D. Arcos, I. Izquierdo-Barba, O. Terasaki, M. Vallet-Regí, Chem. Mater. 19 (2007) 3455.
[21] M. Arruebo, W.Y. Ho, K.F. Lam, X.G. Chen, J. Arbiol, J. Santamaria, K.L. Yeung, Chem. Mater. 20 (2008) 486.
[22] J. Rosenholm, M. Linden, J. Control. Release 128 (2008) 157.
[23] L. Pasqua, S. Cundari, C. Ceresa, G. Cavaletti, Curr. Med. Chem. 16 (2009) 3054.
[24] G. Wang, A.N. Otuonye, E.A. Blair, K. Denton, Z.M. Tao, T. Asefa, J. Solid State Chem. 182 (2009) 1649.

[25] D.R. Radu, C.Y. Lai, K. Jeftinija, E.W. Rowe, S. Jeftinija, V.S.Y. Lin, J. Am. Chem. Soc. 126 (2004) 13216.
[26] I.I. Slowing, B.G. Trewyn, V.S.Y. Lin, J. Am. Chem. Soc. 128 (2006) 14792.
[27] Z.M. Tao, M.P. Morrow, T. Asefa, K.K. Sharma, C. Duncan, A. Anan, H.S. Penefsky, J. Goodisman, A.K. Souid, Nano Letters 8 (2008) 1517.
[28] I.I. Slowing, C.W. Wu, J.L. Vivero-Escoto, V.S.Y. Lin, Small 5 (2009) 57.
[29] M. Vallet-Regí, Chem. Eng. J. 137 (2008) 1.
[30] M. Vallet-Regí, F. Balas, M. Colilla, M. Manzano, Prog. Solid State Chem. 36 (2008) 163.
[31] M. Vallet-Regí, M. Colilla, I. Izquierdo-Barba, J. Biomed. Nanotechnol. 4 (2008) 1.
[32] V. Cauda, S. Fiorilli, B. Onida, E. Verne, C.V. Brovarone, D. Viterbo, G. Croce, M. Milanesio, E. Garrone, J. Mater. Sci.: Mater. Med. 19 (2008) 3303.
[33] R. Mortera, B. Onida, S. Fiorilli, V. Cauda, C.V. Brovarone, F. Baino, E. Verne, E. Garrone, Chem. Eng. J. 137 (2008) 54.
[34] C. Vitale-Brovarone, F. Baino, M. Miola, R. Mortera, B. Onida, E. Verne, J. Mater. Sci.: Mater. Med. 20 (2009) 809.
[35] T. Kokubo, H. Takadama, Biomaterials 27 (2006) 2907.
[36] L.E. Dahners, B.H. Mullis, J. Am. Acad. Orthop. Surg. 12 (2004) 139.
[37] M. Fransen, C. Anderson, J. Douglas, S. MacMahon, B. Neal, R. Norton, M. Woodward, I.D. Cameron, R. Crawford, S.K. Lo, G. Tregonning, M. Windolf, Br. Med. J. 333 (2006) 519.
[38] M. Ahola, P. Kortesuo, I. Kangasniemi, J. Kiesvaara, A. Yli-Urpo, Int. J. Pharm. 195 (2000) 219.
[39] T. Czuryszkiewicz, J. Ahvenlammi, P. Kortesuo, M. Ahola, F. Kleitz, M. Jokinen, M. Linden, J.B. Rosenholm, J. Non-Cryst. Solids 306 (2002) 1.
[40] J.D. Bass, D. Grosso, C. Boissiere, E. Belamie, T. Coradin, C. Sanchez, Chem. Mater. 19 (2007) 4349.
[41] M. Vallet-Regí, Chem. Eur. J. 12 (2006) 5934.
[42] R. Mortera, S. Fiorilli, E. Garrone, B. Onida, Stud. Surf. Sci. Catal. B 174 (2008) 1001.
[43] M. Grün, K.K. Unger, A. Matsumoto, K. Tsutsumi, Micropor. Mesopor. Mater. 27 (1999) 207.
[44] J.B. Mullin, J.P. Riley, Anal. Chim. Acta 12 (1955) 162.
[45] M. Thommes, R. Kohn, M. Froba, Appl. Surf. Sci. 196 (2002) 239.
[46] F. Di Renzo, A. Galarneau, P. Trens, F. Fajula, in: F. Schüth, K. Sing, J. Weitkamp (Eds.), Handbook of Porous Materials, Wiley–VCH, 2002, p. 1311.
[47] M.V. Landau, S.P. Varkey, M. Herskowitz, O. Regev, S. Pevzner, T. Sen, Z. Luz, Micropor. Mesopor. Mater. 33 (1999) 149.
[48] E. Prouzet, F. Cot, G. Nabias, A. Larbot, P. Kooyman, T.J. Pinnavaia, Chem. Mater. 11 (1999) 1498.
[49] P.J. Li, K. Nakanishi, T. Kokubo, K. Degroot, Biomaterials 14 (1993) 963.
[50] P.J. Li, I. Kangasniemi, K. Degroot, T. Kokubo, A.U. Yliurpo, J. Non-Cryst. Solids 168 (1994) 281.
[51] M. Colilla, M. Manzano, M. Vallet-Regí, Int. J. Nanomed. 3 (2008) 403.
[52] S.S. Huang, P.P. Yang, Z.Y. Cheng, C.X. Li, Y. Fan, D.Y. Kong, J. Lin, J. Phys. Chem. C 112 (2008) 7130.
[53] A. Hillerstrom, J. van Stam, M. Andersson, Green Chem. 11 (2009) 662.
[54] A. Ramila, R.P. Del Real, R. Marcos, P. Horcajada, M. Vallet-Regí, J. Sol-Gel Sci. Technol. 26 (2003) 1195.
[55] E.M. Renkin, F.E. Curry, in: G. Giebisch, D.C. Tosteson, H.H. Ussing (Eds.), Membrane Transport in Biology, vol. IV, Springer Verlag, Berlin, 1979.
[56] M. Gibaldi, D. Perrier, Pharmacokinetics, Drugs and the Pharmaceutical Sciences, vol. 15, Marcel Dekker, Inc., New York, 1982.
[57] N.V. Mulye, S.J. Turco, Drug Dev. Ind. Pharm. 21 (1995) 943.
[58] P. Costa, J.M.S. Lobo, Eur. J. Pharm. Sci. 13 (2001) 123.
[59] J. Crank, The Mathematics of Diffusion, 2nd ed., Oxford University Press, Oxford, 1975.
[60] C. Amatore, Chem. Eur. J. 14 (2008) 5449.